TRANSDUCERS '91: 1991 International Conference on Solid-State Sensors and Actuators,
Digest of Technical Papers, Pg: 538 - 542

On the resonance frequencies of microbridges

Siebe Bouwstra and Bert Geijselaers*

MESA, Institute
for Micro-Electronics, Materials Engineering and Sensors and Actuators
**Faculty of Mechanical Engineering*
University of Twente, P. O. Box 217, 7500 AE Enschede, The Netherlands

Abstract

This paper presents the exact analysis of the natural frequencies of transverse bending of flat clamped-clamped beams subject to an axial force. Extensions of this model are presented for several aspects of transversely vibrating microbridges for which this model falls short. The behaviour of buckled or initially deflected beams is modeled, as well as the behaviour of beams with a small length-to-width ratio. The deformation of the elastic support is analyzed, revealing a significant compliance of the support compared relative to typical compliances of microbridges. The results of these models are compared with the experimental results obtained from a resonating microbridge mass flow sensor.

Introduction

Several present-day solid-state sensors are based on the shift of the resonance frequency of a micromechanical structure [1, 2]. The vibrating structure usually consists of single crystal silicon or of a thin film. The supported edges of the microstructure are attached to the substrate, with the geometry of the microstructure and of the supports determined by the applied technology. Ideally, these microstructures would be flat, and the supports would be rigid. Also, it is usually assumed that the lowest natural frequencies can be described by one-dimensional models. The actual geometries, however, affect the mechanical behaviour of these microstructures. This paper takes microbridges as an example, and investigates their natural frequencies as a function of the actual applied load, in relation to their actual geometry.

Clamped-clamped beam model

Ideally, the considered mechanical behaviour of the microbridge can be described by a one-dimensional model for a homogeneous, prismatic beam, clamped at both ends, and subject to an axial force. The free, undamped transverse vibration at small amplitudes can be described by the following linear partial differential equation [3]:

$$\hat{E}I\cdot\partial^4 w/\partial x^4 - N\cdot\partial^2 w/\partial x^2 = -\rho A\cdot\partial^2 w/\partial t^2 \qquad (1a)$$

with boundary conditions:

$$w|_{x=0,l} = 0 \text{ and } \partial w/\partial x|_{x=0,l} = 0 \qquad (1b)$$

In eqn. (1) $w(x,t)$ is the dynamic transverse deflection of the beam, see figure 1, with x for axial position and t for time, $\hat{E}$ is the Young modulus, N the axial tensile force and ρ the density of the beam material; A and I are the area and moment of inertia of the cross section of the beam, respectively ($A = b\cdot h$ and $I = b\cdot h^3/12$ for rectangular cross-sections, with b and h the width and thickness, respectively). For non-homogeneous, but still prismatic beams, eqn. (1) is still valid, if the coefficients for the flexural rigidity $\hat{E}I$ and the mass per unit length ρA are properly defined for the non-homogeneous cross section, and if the neutral axis does not have steps. For a rectangular cross section with ratio $b/h > 5$, $\hat{E}$ in equation (1a) should be replaced by $E/(1-\nu^2)$, with E the Young modulus and ν the Poisson ratio, to account for the suppresion of the in-plane dilation accompanying axial strain [4]. In the case of anisotropic elastic behaviour the appropriate values for E and ν can be determined from the appropriate stress-strain relations.

The axial force N can be caused by a displacement u of the clamped ends relative to each other, $N = EA\epsilon$, $\epsilon = u/l$. A contribtution to the axial force N due to the bi-axial residual stress σ_0 can be found from $N = (1-\nu)\cdot\sigma_0 A$.

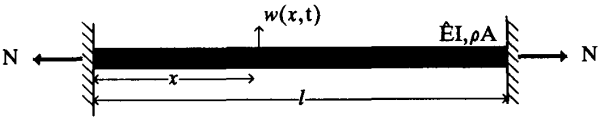

Figure 1. Transverse deflection $w(x,t)$ of a clamped-clamped beam with flexural rigidity $\hat{E}I$, mass per unit length ρA and length l, subject to an axial tensile force N.

The solution of equation (1) can be written [3]:

$$w(x,t) = \sum_n \chi_n(\tfrac{x}{l})\cdot(A_n\cdot\cos\omega_n t + B_n\cdot\sin\omega_n t) \qquad (2)$$

with ω_n the radial frequency, and χ_n the shape function of the n-th natural mode. With eqn.(2) Eqn.(1) can be rewritten:

$$\chi_n'''' - 2\beta\cdot\chi_n'' - k_n^4\cdot\chi_n = 0 \qquad (3a)$$

$$\chi_n|_{\eta=0,1} = 0,\ \chi_n'|_{\eta=0,1} = 0 \qquad (3b)$$

where $'$ denotes derivation with respect to $\eta = x/l$, $k_n^4 = \rho A\omega_n^2 l^4/\hat{E}I$ and $2\beta = Nl^2/\hat{E}I$. Substituting the general solution of (3a) into (3b) yields [5]:

$$\chi_n = \frac{\cosh\kappa_{2n}\eta - \cos\kappa_{1n}\eta}{\cosh\kappa_{2n} - \cos\kappa_{1n}} - \frac{\sinh\kappa_{2n}\eta - \sin\kappa_{1n}\eta}{\sinh\kappa_{2n} - \sin\kappa_{1n}} \qquad (4a)$$

$$\cos\kappa_{1n}\cdot\cosh\kappa_{2n} - (\beta/k_n^2)\cdot\sin\kappa_{1n}\cdot\sinh\kappa_{2n} - 1 = 0 \qquad (4b)$$

$$\kappa_{in} = ((k_n^2 + \beta^2)^{1/2} + (-1)^i\beta)^{1/2},\ i = 1, 2. \qquad (4c)$$

The exact natural radial frequencies as a function of the axial force $\omega_n = k_n^2\cdot(\hat{E}I/\rho Al^4)^{1/2}$ are found from from the solutions $k_n(\beta)$ of the implicit equation (4b). Figure 2 shows a graphical representation of the two lowest exact solutions $\nu_n = \omega_n/2\pi$ of eqn. (1) as a function of the applied axial force. Note that thanks to the normalization of the frequencies (with ν_0 the value of ν_1 at zero axial force), and of the force the graph is generally applicable. These exact solutions can be approximated by a closed form relation:

$$\nu_n(N) = \nu_n(0)\cdot\sqrt{(1 + \gamma_n\cdot\frac{Nl^2}{12\hat{E}I})} \qquad (5)$$

where γ_n is a coefficient for the contribution of the applied axial force to the modal stiffness, relative to the contribution of the flexural rigidity. Values for k_n and ν_n/ν_0 at zero axial force, and for the coefficient γ_n in eqn. (5) are listed in table 1. The error in the approximation is smaller than 0.5 % if the contribution of the axial force to the modal stiffness is smaller than that of the flexural rigidity, *i.e.*, $\gamma_n\cdot Nl^2/(12\hat{E}I) < 1$.

For the buckling value of the axial force, *i.e.*, for $N = -N_b$, with $N_b = 4\pi^2\hat{E}I/l^2$, a zero frequency is found for the first natural mode, while $\nu_2 = 1.98\cdot\nu_0$. For larger compressive forces, the structure is buckled, and the model is not adequate.

91CH2817-5/91/0000-0538$01.00 © 1991IEEE

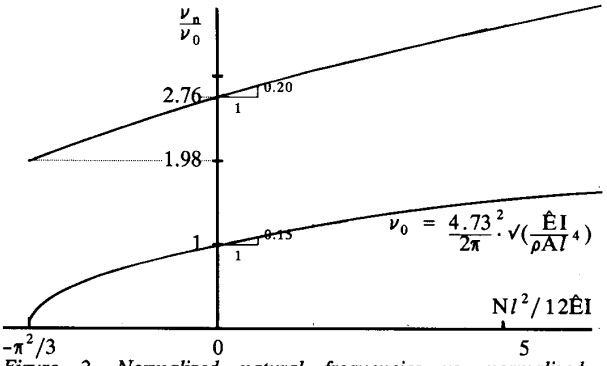

Figure 2. Normalized natural frequencies vs. normalized axial force [5]. For homogeneous rectangular cross sections $Nl^2/12\hat{E}I = N/EA\cdot(l/h)^2(1-\nu^2)$, $\nu_0 = 1.028\cdot\sqrt{(\hat{E}/\rho)}\cdot(h/l^2)$.

Effects of shear deformation and of rotational inertia were omitted in the above analysis. This is valid for $(k_n h/l)^2 \ll 1$ [3]. For large amplitudes of vibration and suppression of axial displacement of the clamped ends, an additional term emerges in equation (1a) due to dynamic elongation of the beam. This leads to a non-linear differential equation. The relative increase of the natural frequencies due to the influence of the amplitude of vibration is of the order $(w_{max}/h)^2$. Also omitted in eqn. (1a) are damping, an additional effective inertia of surrounding medium and a provisional transverse force with a gradient in the direction of vibration. These phenomena have a decreasing effect on the actual resonance frequencies. For non-prismatic beams it is convenient to use an approximation method, rather than solving the differential equation.

n	k_n	ν_n/ν_0	γ_n
1	4.7300	1.0000	0.2949
2	7.8532	2.7566	0.1453
≥3	$(n+1/2)\pi$	$(\frac{k_n}{4.73})^2$	$\frac{12(k_n-2)}{k_n^3}$

$\nu_0 = \frac{4.73^2}{2\pi}\cdot\sqrt{(\frac{\hat{E}I}{\rho A l^4})}$

Table 1. Values for the coefficients in eqn. (5). k_n *and* ν_n *for* N=0.

Buckled beam model

To investigate the behaviour of buckled microbridges, it is better to regard the axial displacement as the input load, rather than the axial force. (Note: most resonant sensors are in fact displacement sensors rather than force sensors.) Kim and Dickinson [6] presented a model for the static behaviour and for the natural frequencies of beams with a small initial deflection, subject to an axial end displacement of the clamped ends. Figure 3 shows a schematic representation of the deflected shapes with and without the axial load, respectively. The axial displacement u causes a uni-axial elastic elongation of the beam corresponding to the actual axial force N, together with a change in projected length of the deflected shape:

$$u = Nl/EA + \int_0^l 1/2\cdot(z'(x))^2dx - \int_0^l 1/2\cdot(y'(x))^2dx$$

where $z(x) = z\cdot\psi(x)$ and $y(x) = y\cdot\psi(x)$, with z and y the centre deflection of the unloaded and loaded beam, respectively. Approximating the deflected shape with $\psi(x) = (1-\cos 2\pi x/l)/2$ this yields:

$$u/l = N/EA + (\frac{\pi z}{2l})^2 - (\frac{\pi y}{2l})^2 \qquad (6a)$$

while $y = z/(1+N/N_b)$, with $N_b = 4\pi^2\hat{E}I/l^2$ [6], except for $z = 0$, $u/l < -\epsilon_b$, with $\epsilon_b = N_b/EA$, for which:

$$N = -N_b \text{ and } (\frac{\pi y}{2l})^2 = -u/l - \epsilon_b \qquad (6b)$$

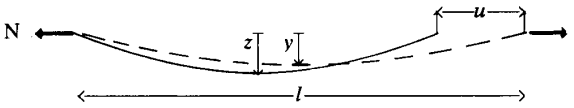

Figure 3. Shape and centre deflection z and y of initially deflected beam without and with axial loading, respectively.

Figure 4 shows graphical representations of eqns. (6). For an initially flat microbridge ($z = 0$) the centre deflection is zero and the stress is proportional to the strain, for values of the axial displacement larger than the buckling value (*i.e.*, $u/l > -\epsilon_b$). For negative values of u/l beyond the buckling point, however, the initially flat microbridge is buckled; the excess length is relaxed by an increase of the centre deflection rather than an increase of the stress. According to the model presented in reference [6] the axial stress does not change with compressive axial displacements beyond the buckling value. Figure 4 shows dashed lines for several initial centre deflections z, again according to the model in reference [6]. When the beam is in a transverse vibration, buckling is enhanced; the amplitude of vibration has a similar impact as an initial static deflection. A step in the neutral axis of a non-prismatic beam has the same effect as an initial deflection $z(x)$. The initial deflection may also be enhanced by a transverse load. Although a small initial deflection has a small impact on the force-displacement curve, and its impact on the deflection-displacement curve is also small, the combined impact can be significant near the buckling point.

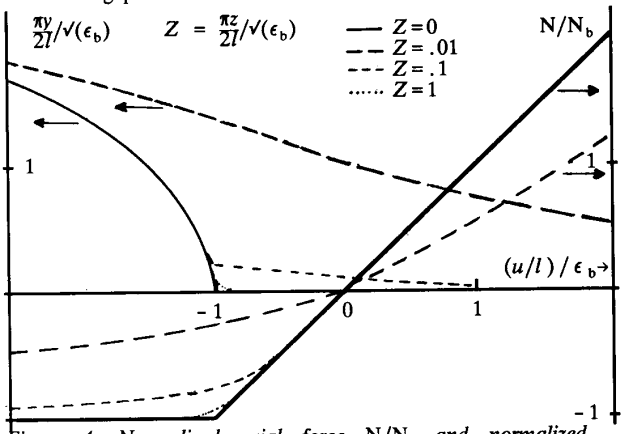

Figure 4. Normalized axial force N/N_b *and normalized transverse deflection* $(\pi/2)(y/l)/\sqrt{\epsilon_b}$ *as a function of normalized axial displacement* $u/(l\epsilon_b)$, *for four values of the normalized initial deflection* Z *[6]. For homogeneous rectangular cross sections* $\epsilon_b = (\pi^2/3)\cdot(h/l)^2(1-\nu^2)$, $N/N_b = 0.304\cdot N/\hat{E}A\cdot(l/h)^2$, $Z = 0.866\cdot z/h\cdot\sqrt{(1-\nu^2)}$ *etc.*

When a statically deflected beam vibrates, a dynamic axial force $N(t) = EA\cdot\int 1/2\cdot((y'+w')^2-(y')^2)dx/l$ occurs due to dynamic stretching of the beam. For small amplitudes of vibration only the part linear in $w(x)$ is significant, leading to the partial differential equation for the undamped free vibration of a statically deflected beam:

$$\hat{E}Iw'''' - Nw'' - EA\cdot\frac{1}{l}\int_0^l y'w'dx\cdot y'' - \rho A\omega^2 w = 0 \qquad (7)$$

where y and N are the actual static centre deflection and axial force, respectively, and where $w(x)$ satisfies the boundary conditions as in eqn. (1b). Ref. [5] uses the Galerkin method, approximating the solution $w(x)$ with a series of the exact mode shapes of initially flat clamped-clamped beams as in eqn. (4), under zero axial

stress. Figure 5 gives a graphical representation of the normalized first two bending modes as a function of normalized axial displacement, and for different values of the initial deflection. For $-1.3 < (u/l)/\epsilon_b < 1$ the curves in figure 5 are well aproximated by:

$$\frac{\nu_1}{\nu_0} = \sqrt{(1 + 0.295\cdot\frac{Nl^2}{12\hat{E}I} + 0.12\cdot\frac{EAy^2}{\hat{E}I})} \quad (8a)$$

$$\frac{\nu_2}{\nu_0} = 2.76\cdot\sqrt{(1 + 0.145\cdot\frac{Nl^2}{12\hat{E}I})} \quad (8b)$$

where y and N are functions of the initial deflection and of the axial displacement, from eqn. (6) and figure 4.

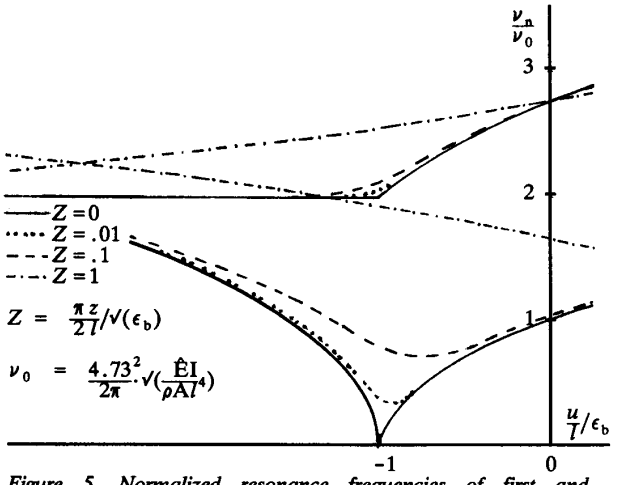

Figure 5. Normalized resonance frequencies of first and second bending modes ν_n/ν_0 as a function of normalized axial displacement $u/(l\epsilon_b)$ including the effect of buckling, for several values of the normalized initial deflection Z [6].

From eqns. (8) it is seen that the influence of the axial force is the same as in eqns. (5). An additional term with the actual deflection y has emerged in the equation for the first bending mode resonance frequency. The second mode natural frequency is not directly affected by the deflection due to the orthogonality of the symmetric deflection shape and the anti-symmetric vibration shape. This behaviour implies that if the resonating beam serves as a force sensor rather than as a displacement sensor, it may be preferable to operate the beam at the second bending mode rather than the first mode.

For a buckled, initially flat beam ($z = 0$), the contributions to the modal stiffness of the first bending mode by the flexural rigidity and by the axial compressive force compensate each other, and the solution can be approximated with:

$$\frac{\nu_1}{\nu_0} = 1.4\cdot\sqrt{(-\frac{u}{l}/\epsilon_b - 1)} \quad (9a)$$

for $-1.3 < (u/l)/\epsilon_b < -1$, while the second mode resonance frequency is independent of compressive axial displacement beyond the buckling point:

$$\frac{\nu_2}{\nu_0} = 1.98 \quad (9b)$$

Again, the approximations in eqns. (8) and (9) are upper limits for the exact solutions for the resonance frequencies. For initially deflected beams the value of ν_2 approaches that of eqn. (9b) for large compressive axial displacements, so that the value of ν_0 of a microbridge can always be determined from eqn. (9b) with a simple experiment. The value of the initial deflection z can then be determined from the minimum value of the measured curve for ν_1/ν_0. From the curves in figure 5 it can be deduced that this minimum is proportional to the cubic root of the normalized initial deflection. For beams with a rectangular cross section the minimum in the (ν_1/ν_0)-curve roughly equals $1.5\cdot(z/h)^{1/3}$.

Two-dimensional analysis

Micromechanical structures usually have a width which is of the same order of magnitude as their length. For these geometries the resonance frequencies of torsional modes may be of the same order of magnitude [7]. Also, the natural frequencies of the bending modes may be slightly smaller than those according to the one-dimensional model, due to anti-clastic bending [8]. A two-dimensional model is required to analyse the behaviour of these beams. Figure 6 shows a graphical representation of results obtained from an ANSYS finite element calculation using shell elements. The structure was given a small centre deflection, $z/h = 0.01$, which was necessary to allow for calculations beyond the buckling load. It shows that for length to thickness ratios of 2, 3 and 4 the resonance frequencies of the first torsional mode is in the same range as those of the two first bending modes. According to ref. [8] the natural frequencies of the bending modes should have a small dependence on the length to width ratio of up to 1 % in this region. However, this dependence was not found in these FEM results.

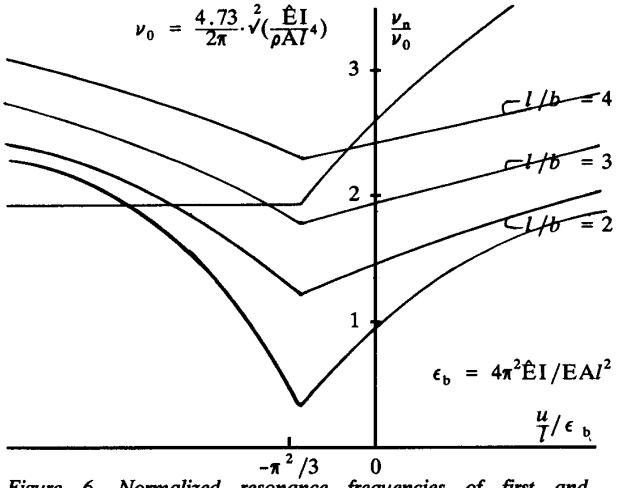

Figure 6. Normalized resonance frequencies of first and second bending modes, as well as of first torsional mode [7], parameterized for length-to-width ratio, as a function of normalized axial displacement.

Elastic supports

In the above models it was assumed that the beams were ideally clamped at both ends. Micromechanical beams, however, are attached to an elastic support. For the analysis of the deformation of the support we make use of the 2-dimensional model in [9] for the deformation of a wedge of angle 2α, under the combined loading of forces P and Q and bending moment M_0 at the tip of the wedge, as in figure 7a. At first instance we will assume the support to have a width equal to that of the beam, and we will assume plane strain, *i.e.*, suppression of strain perpendicular to the plane of the wedge. This implies that below E and ν should be read $E/(1-\nu^2)$ and $\nu/(1-\nu)$, respectively.

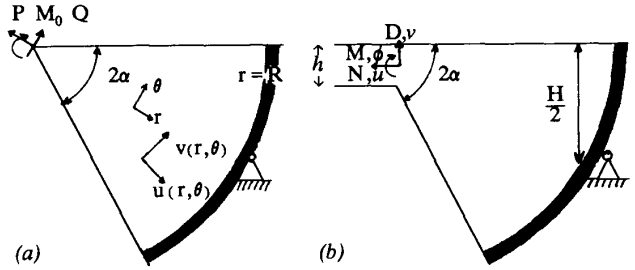

Figure 7. Wedge loaded at its tip (a), and elastic support of beam loaded at the height of the neutral axis of the beam (b).

The stress distributions are according to [9]:

$$\sigma_r = \frac{P\cos\theta}{brf_P(\alpha)} - \frac{Q\sin\theta}{brf_Q(\alpha)} - \frac{M\sin2\theta}{br^2f_m(\alpha)}$$

$$\sigma_\theta = 0 \qquad (10)$$

$$\tau_{r\theta} = \frac{M(\cos2\theta-\cos2\alpha)}{2br^2f_m(\alpha)}$$

with $f_P(\alpha) = \alpha + 1/2\cdot\sin2\alpha$
$f_Q(\alpha) = \alpha - 1/2\cdot\sin2\alpha$
$f_m(\alpha) = 1/2(\sin2\alpha - 2\alpha\cos2\alpha)$

Substituting eqns. (10) into the constitutive equations yields expressions for the strains as functions of r and θ. The displacements can be found from integration of the strain-displacement expressions: $\epsilon_r = \partial u/\partial r$, $\epsilon_\theta = u/r + \partial v/r\partial\theta$, $\gamma_{r\theta} = \partial u/r\partial\theta + \partial v/\partial r - v/r$. Assuming zero-displacements at distance R from the tip of the wedge, this yields for the displacements at the axis $\theta=0$:

$$u(r) = \frac{P}{bE}\cdot\frac{1}{f_P(\alpha)}\cdot\ln(R/r)$$

$$v(r) = \frac{Q}{bE}\cdot\frac{1}{f_Q(\alpha)}\cdot(\ln(R/r)-(1-r/R)) + \frac{M}{brE}\cdot\frac{1}{f_M(\alpha)}\cdot(1-r/R)^2 \qquad (11)$$

$$\phi(r) = -\frac{\partial v}{\partial r} = \frac{Q}{brE}\cdot\frac{1}{f_Q(\alpha)}\cdot(1-r/R) + \frac{M}{br^2E}\cdot\frac{1}{f_M(\alpha)}\cdot(1-(r/R)^2)$$

with $f_M(\alpha) = f_m(\alpha)/(1 - (1+\nu)(1-\cos2\alpha)/2)$

For small angles 2α the same results are obtained as in eqns. (11) if the wedge is regarded as a non-prismatic beam of thickness $h(x) = 2x\tan\alpha$, and applying a one-dimensional model of deformation by axial elongation, bending and shear.

An appropriate point to evaluate eqns. (11) is the point at the height of the neutral axis of the beam, *i.e.* where $r = (h/2)/\sin\alpha$. For radius R we can define $R = (H/2)/\sin\alpha$, where H is a characteristic dimension, *e.g.* the distance to a rigid backplate. Replacing loads P, Q and M_0 by loads N, D and M enacted at the height of the neutral axis of the beam: $P = N\cos\alpha + D\sin\alpha$, $Q = D\cos\alpha - N\sin\alpha$, $M_0 = M - N\cdot r\sin\alpha + D\cdot r\cos\alpha$ and expressing the displacements in the components u, v and ϕ as in figure 7b, we find:

$$\begin{bmatrix} u \\ v \\ \phi h \end{bmatrix} = S\cdot\begin{bmatrix} N/bE \\ D/bE \\ M/bhE \end{bmatrix} \qquad (12)$$

$$S = \begin{bmatrix} c^2\cdot\chi_P + s^2\cdot\chi_Q - s^2\cdot\chi_M & sc\cdot\chi_P - sc\cdot\chi_Q + sc\cdot\chi_M & -2s^2\cdot\chi_M \\ sc\cdot\chi_P - sc\cdot\chi_Q + sc\cdot\chi_M & s^2\cdot\chi_P + c^2\cdot\chi_Q - c^2\cdot\chi_M & 2sc\cdot\chi_M \\ -2s^2\cdot\chi_Q' + 2s^2\cdot\chi_M' & 2sc\cdot\chi_Q' - 2sc\cdot\chi_M' & 4s^2\cdot\chi_M' \end{bmatrix}$$

where $c = \cos\alpha$, $s = \sin\alpha$, $\chi_X = g_X/f_X$, with g_X according to eqn. (11):

$$g_P = \ln\frac{H}{h},\ g_Q = \ln\frac{H}{h} - (1-\frac{h}{H}),\ g_M = (1-\frac{h}{H})^2,\ g_Q' = 1-\frac{h}{H},\ g_M' = 1-(\frac{h}{H})^2$$

and with f_X from eqns. (10). As the matrix S has to be symmetric it turns out that probably the expression for f_M in eqn. (11) is wrong, and should be replaced by $f_M = 2f_Q$. Results of the above analysis agree with results obtained from FEM calculations.

In reality the loads P, Q and M_0 will decrease with increasing depth into the support, as they are counterbalanced by the bulk surrounding the wedge. If we assume $P(r) = P/(1+r/b)$, $M(r) = (M_0+Qr)/(1+r/b)$, we obtain for $H > 10\cdot b$, and replacing b/r by b/h in the expressions for g_X:

$$g_P = \ln(1+\frac{b}{h}),\ g_Q = (1+\frac{h}{b})\ln(1+\frac{b}{h}) - 1,\ g_Q' = 1 - \frac{h}{b}\ln(1+\frac{b}{h})$$

$$g_M = 1 - 2\frac{h}{b}(1+\frac{h}{b})\ln(1+\frac{b}{h}),\ g_M' = 1 - 2\frac{h}{b} + 2(\frac{h}{b})^2\ln(1+\frac{b}{h})$$

Table 2 gives values of the coeffients of the compliance matrix S for $b/h = 100$, and for three different values of 2α.

$2\alpha = 54.7°$	$2\alpha = 90°$	$2\alpha = 144.7°$
13.9 -16.8 -2.8	7.4 -3.8 -1.6	1.7 0.4 -0.8
-16.8 37.6 5.3	-3.8 7.4 1.6	0.4 2.8 0.3
-2.8 5.4 6.0	-1.6 1.6 3.4	-0.9 0.3 1.8

Table 2. Values of coefficients of the compliance matrix of the support, for b/h = 100, and for different values of 2α.

The coefficient s_{11} represents the axial diplacement of the elastic support under an axial load. For this load the support can be regarded as a spring in series with the beam, see figure 8a. The value of s_{11} should be compared with the axial compliance of the beam, *i.e.*, $0.5(l/h)$. For l/h = 100, 200 or 300, the values of the latter are only a few times higher than those in table 2, indicating that the support is not relatively stiff for this load. Even for the support of an angle of 144.7°, and a beam with l/h = 300, the axial force due to an axial diplacement is 1 % less than would have been the case for a rigid support. For 2α = 54.7° and l/h = 100 the axial force is even 22 % smaller.

The coefficient s_{12} represents the transverse displacement of the end of the beam due to deformation of the support under an axial load. A static transverse diplacement, however, is irrelevant, and we will ignore the dynamic transverse displacement due to this effect.

The value of the coefficient s_{13} represents the angle of rotation ϕ of the support under the axial force N. This causes a deflection $z = \phi\cdot l/4$ at the centre of the beam, see figure 8b. This contribution to the initial deflection of the beam, which is proportional to the axial load, is particularly interesting for the buckling load of the beam, because, as we have found earlier, the effect of the initial deflection on the resonance frequency is largest around the buckling load. The value of the normalized initial deflection z/h under the buckling load, due to deformation of the elastic support, can be found by multiplying the coefficient s_{13} by $\pi^2/12\cdot(h/l)$. For 2α = 144.7° and l/h = 300 this centre deflection due to the buckling load equals z/h = 0.002, while for 2α = 54.7° and l/h = 100 z/h = 0.023, which is quite significant. (Note that for a symmetric support the rotation would be zero.)

The coefficients s_{21} and s_{31} represent the dynamic axial elongation of the beam, see figure 8c, in the case of a transverse vibration, due to deformation of the support under the actual tranverse force and bending moment at the end of the beam. These loads are caused by the inertial forces of the beam during the vibration, and can be found from derivatives of the modal shape functions: $M(t) = EIw''(0,t)$, $D(t) = EIw'''(0,t)$. For values of $(k_n h/l) < 1$ the axial displacement of the support is dominated by that due to the bending moment, $u = s_{31}/12\cdot(k_n h/l)^2 w(l/2,t)$. This dynamic axial displacement is counterbalanced by an axial force similar to that in eqn. (7), and therefore will only show up in the differential equation in the presence

of a static deflection y of the beam, and it will show up as a cross term of s_{31} and y in eqn. (8). To compare the value of the dynamic axial elongation due to deformation of the support, with that due to a static deflection of the beam as in eqn. (7) (which is proportional with y/l), the coefficient s_{31} should be multiplied by $(k_n h/l)^2/12$. The equivalent normalized centre deflection y/h is then found from: $y/h = s_{31} \cdot k_n^2 (h/l)/12$. For $l/h = 300$, $k_n = 4.73$ and $2\alpha = 144.7°$ this yields $y/h = 0.005$, while for $l/h = 100$, $k_n = 4.73$ and $2\alpha = 54.7°$ this yields $y/h = 0.05$, which is again quite significant according to figure 5.

The coefficients s_{22}, s_{23}, s_{32} and s_{33} represent transverse deflections and angles of rotation of the clamped edges due to a transverse force D and a bending moment M. The compliances of the elastic support to these loads can be expressed in an equivalent prismatic extension of the beam of length Δl, ideally clamped at its end, see figure 8d. The value of Δl can be found from the expressions for bending of the extension: $\phi = M\Delta l/EI + D(\Delta l)^2/2EI$, $v = M(\Delta l)^2/2EI + D(\Delta l)^3/3EI$. For natural vibrations of the beam with $(k_n h/l) < 1$, the transverse force D is relatively small compared to the bending moment M, *i.e.*, the deformation of the support is dominated by the impact of the bending moment. Therefore we only have to look for an extension Δl equivalent to the coefficients s_{32} and s_{33}. To define one characteristic value of Δl we take the average of the equivalent compliances for ϕ and v:

$$\Delta l = 1/2(s_{33}/12 + (s_{32}/6)^{1/2}) \cdot h$$

We see that the equivalent extension is proportional to the thickness of the beam. The complete structure of beam of length l together with the elastic supports at both ends can now be regarded as an equivalent clamped-clamped beam with length $l + 2\Delta l$. For $2\alpha = 144.7°$ we find $2\Delta l = 0.37 \cdot h$, for $2\alpha = 90°$ $2\Delta l = 0.80 \cdot h$, and for $2\alpha = 54.7°$ $2\Delta l = 1.44 \cdot h$. For $l/h = 300$ an extension of the beam length of $0.37 \cdot h$ leads to a decrease of frequency ν_0 by 0.25 %. For $l/h = 100$ an extension of the beam length of 1.44 leads to a decrease of ν_0 of 2.8 %, which is again significant. The shift of the resonance frequency due to an axial force is not affected by the extension of the beam length, for small values of the axial force.

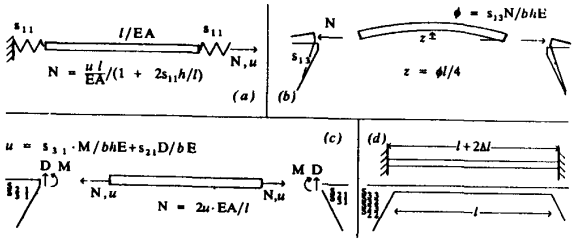

Figure 8. Schematic representations of the effects of the finite stiffness of the elastic support (a) series spring effect for axial displacement, (b) initial deflection due to static rotation of support under axial force, (c) dynamic axial loading of the beam due to dynamic axial displacement of the support, and (d) equivalent extension of the beam length due to rotation and transverse deflection of the support.

Discussion and conclusions

The analysis of the behaviour of beams with an initial deflection shows that the latter has a considerable effect on the relationship between axial displacement and the resonance frequency of the first bending mode, especially near the buckling load of the beam. The prevailing parameter is the ratio between initial deflection and thickness of the beam. The latter is usually of the order of microns for micromechanical structures. The relationship between the resonance frequencies of antisymmetric modes and the actual axial force is independent of the initial deflection.

The two-dimensional analysis of the natural vibrations of the beams show that for a beam with a width of the same order of magnitude as its length the natural frequency of the first torsion mode is of the same order of magnitude as those of the first bending modes.

The analysis of the elastic support shows that the support is reasonably stiff compared to the stiffness of the beam against bending, but not compared to the stiffness of the beam against axial elongation. Effects of the finite stiffness of the support are considerable for supports of a small angle ($2\alpha < 90°$) and for beams with a small length to thickness ratio (*e.g.*, $l/h = 100$). Due to the deformation of the support, an axial elongation of the beam relative to the (far away) substrate leads to a smaller axial force than in the case of a rigid support. Rotation of the support even leads to an initiitial deflection of the beam proportional to the axial force. Its impact on the resonance frequency can be considerable, especially near the buckling load of the beam. Also for loads due to vibrations of the beam the deformation of the support is considerable, leading to smaller resonance frequencies.

These analyses reasonably well explain the experimental results obtained for a resonating microbridge mass flow sensor [10]. The experimental resonance frequency - temperature elevation curves indicate an equivalent initial deflection to thickness ratio of 0.02 to 0.05.

Acknowledgements

The research of Dr. Siebe Bouwstra has been made possible by a fellowship of the Royal Netherlands Academy of Arts and Sciences. The authors would like to thank Harrie A. C. Tilmans for his comments on the manuscript.

References

[1] R. T. Howe, Resonant Microsensors, *Proc. Int. Conf. Solid-State Sensors & Actuators (Transducers '87), Tokyo, Japan, June 1987*, pp. 843-848.

[2] J. C. Greenwood, Silicon Resonant Sensors, invited paper presented at *Int. Conf. Solid-State Sensors & Actuators (Transducers '89), Montreux, Switzerland, June 1989.*

[3] S. P. Timoshenko, D. H. Young and W. Weaver, *Vibration problems in engineering*, Ch. 5, 4th edn., John Wiley & Sons (1974).

[4] S. P. Timoshenko and S. Woinowski-Krieger, *Theory of Plates and Shells*, 2nd edn., McGraw-Hill Book Co. (1970), pp. 1.

[5] W. C. Albert, Vibrating Quartz Crystal Beam Accelerometer, Proc. 28th ISA Int. Instrument. Symp., Las Vegas, NV, USA, May 1982, pp. 33-44.

[6] C. S. Kim and S. M. Dickinson, The flexural vibration of slightly curved lsender beams subject to axial end displacement, *J. Sound and Vibration, 104* (1986) 170-175.

[7] B. Geijselaers and H. Tijdeman, The dynamic mechanical characteristics of a resonating microbridge mass flow sensor, accepted for publication in *Sensors and Actuators*, February 1991.

[8] R. D. Blevins, *Formulas for Natural Frequency and Mode Shape*, Van Nostrand Reinhold, 1979, pp. 183.

[9] S. P. Timoshenko and J. N. Goodier, *Theory of Elasticity*, McGraw-Hill Book Co., 3rd edn. (1982) pp. 109-113.

[10] S. Bouwstra, *Resonating Microbridge Mass Flow Sensor*, Ph. D. thesis, University of Twente, March 1990, ISBN 90-900 3328-9. See also: S. Bouwstra, R. Legtenberg and T. J. A. Popma, Response of resonating microbridge mass flow sensor, submitted to *IEEE Transactions on Electron Devices*, November 1990.